# Optical and Infrared Observations of the X-ray source 1WGA J1713.4−3949 in the G347.3-0.5 SNR[*]

R. P. Mignani[1], S. Zaggia[2], A. De Luca[3], R. Perna[4], N. Bassan[3], and P. A. Caraveo[3]

[1] Mullard Space Science Laboratory, University College London, Holmbury St. Mary, Dorking, Surrey, RH5 6NT, UK
   e-mail: rm2@mssl.ucl.ac.uk
[2] INAF, Osservatorio Astronomico di Padova, Vicolo dell'Osservatorio 5, Padua, 35122, Italy
   e-mail: simone.zaggia@oapd.inaf.it
[3] INAF, Istituto di Astrofisica Spaziale, Via Bassini 15, Milan, 20133, Italy
   e-mail: [deluca,bassan,pat]@iasf-milano.inaf.it
[4] JILA and Department of Astrophysical and Planetary Sciences, University of Colorado, 440 UCB, Boulder, 80309, USA
   e-mail: rosalba@jilau1.Colorado.EDU

## ABSTRACT

*Context.* X-ray observations unveiled the existence of enigmatic point-like sources at the centre of young supernova remnants (SNRs). These sources, dubbed Central Compact Objects (CCOs), are thought to be neutron stars formed by the supernova explosion. However, their multi-wavelength phenomenology is surprisingly different from that of most young neutron stars.
*Aims.* The aim of this work is to understand the nature of the CCO 1WGA J1713.4−3949 in the G347.3-0.5 SNR, through deep optical and IR observations, the first ever performed for this source.
*Methods.* By exploiting its derived *Chandra* X-ray position we carried out optical (BVI) observations with the *NTT* and Adaptive Optics IR ($JHK_s$) observations with the *VLT*.
*Results.* We detected two faint (I≈ 23.5, I≈ 24.3.) patchy objects in the *NTT* images, close to the *Chandra* error circle. They were clearly resolved in our *VLT* images which unveiled a total of six candidate counterparts ($17.8 < H < 20.3$) with quite red colours (H-$K_s$∼0.6). If they are stars, none of them can be associated with 1WGA J1713.4−3949 for the most likely values of distance and hydrogen column density. The identification of the faintest candidate with the neutron star itself can not be firmly excluded, while the identification with a fallback disk is ruled out by its non-detection in the I band. No other candidates are detected down to B∼ 26, V∼ 26.2, I∼ 24.7, H∼21.3 and K∼20.5.
*Conclusions.* Our high-resolution IR imaging of unveiled a few objects close/within the *Chandra* X-ray position of 1WGA J1713.4−3949. However, at present none of them can be firmly identified as its likely counterpart.

**Key words.** Stars: neutron, Stars: individual: 1WGA J1713.4−3949

## 1. Introduction

X-ray observations have unveiled the existence of peculiar classes of Isolated Neutron Stars (INSs) which stand apart from the family of more classical radio pulsars in being radio-silent and not powered by the neutron star rotation but by still poorly understood emission mechanisms. Some of the most puzzling classes of radio-silent INSs are identified with a group of X-ray sources detected at the centre of young (∼ 10-40 kyears) supernova remnants (SNRs), hence dubbed Central Compact Objects or CCOs (Pavlov et al. 2002).

Although the SNR associations imply ages of the order of a few kyears, their X-ray properties make CCOs completely different from the other young INSs in SNRs (Pavlov et al. 2004; De Luca 2008). Oly two of them exhibit X-ray pulsations, with periods in the ∼ 100-400 ms range, and the measured upper limits on the period derivatives yield spin down ages $\geq 10^3$ exceeding the SNR age. Furthermore, their X-ray spectra are not purely magnetospheric but have strong thermal components. Finally, they are not embedded in pulsar wind nebulae (PWN). The discovery of long term X-ray flux variations (Gotthelf et al. 1999) and of a 6.7 hours periodicity (e.g. De Luca et al. 2006) in the RCW 103 CCO further complicated the picture, suggesting either a binary system with a low-mass companion, or a long-period magnetar (De Luca et al. 2006; Pizzolato et al. 2008). For other CCOs, the in-

---

voked scenarios involve low-magnetised INSs surrounded by debris disks formed after the supernova event (Gotthelf & Halpern 2007; Halpern et al. 2007), isolated accreting black holes (Pavlov et al. 2000), and dormant magnetars (Krause et al. 2005). In the optical/IR, deep observations have been performed only for a handful of objects (see De Luca 2008 for a summary) but no counterpart has been identified yet, with the possible exception of the Vela Jr. CCO (Mignani et al. 2007a).

One of the CCOs which still lack a deep optical/IR investigation is 1WGA J1713.4−3949 in the young ($\leq$ 40 kyears) G347.3-0.5 SNR. Discovered by *ROSAT* (Pfeffermann & Aschenbach 1996), the source was re-observed with *ASCA* and identified as an INS due to its high-temperature spectrum and the lack of an optical counterpart (Slane et al. 1999). 1WGA J1713.4−3949 was later observed with *RXTE*, *Chandra* and *XMM* (Lazendic et al. 2003; Cassam-Chenaï et al. 2004), with all the observation consistent with a steady X-ray emission. The X-ray luminosity is $L_{0.5-10keV} \sim 6 \ 10^{34}$ (d/6 kpc)$^2$ erg s$^{-1}$, where 6 kpc is the originally estimated SNR distance (Slane et al. 1999). A revised distance of $1.3 \pm 0.4$ kpc was recently obtained by Cassam-Chenaï et al. (2004). The X-ray spectrum can be fitted either by a blackbody, likely produced from hot polar caps, plus a power-law ($kT \sim$ 0.4 keV; $\Gamma \sim 4$; $N_H \sim 9 \ 10^{21}$ cm$^{-2}$), or by two blackbodies ($kT_1 \sim 0.5$ keV; $kT_2 \sim 0.3$ keV; $N_H \sim 5 \ 10^{21}$ cm$^{-2}$). No X-ray pulsations were detected so far (Slane et al. 1999; Lazendic et al. 2003), nor any radio counterpart (Lazendic et al. 2004), thus strengthening the case for 1WGA J1713.4−3949 to be a member of the CCO class.

Here we present the results of the first, deep optical/IR observations of 1WGA J1713.4−3949 performed with the ESO telescopes. Observations are described in Sect. 2, while the results are described and discussed in Sect 3 and 4, respectively.

## 2. Observations and data reduction

### 2.1. Optical observations

1WGA J1713.4−3949 was observed on June 13th 2004 at the ESO La Silla Observatory with the *New Technology Telescope* (*NTT*). The telescope was equipped with the second generation of the *SUperb Seeing Imager* (*SUSI2*). The camera is a mosaic of two 2000×4000 pixels EEV CCDs with a 2×2 binned pixel scale of 0.″16 (5′.5 × 5′.5 field of view).

Repeated exposures were obtained in the broad-band B, V, and I filters. The *SUSI2* observations log is summarised in the first half of Table 1. Observations were performed with the target close to the zenith and under reasonably good seeing conditions ($\sim 1''$). Since the target was always centred on the left chip, no dithering was applied to the B and V-band exposures while the I-band ones were dithered to compensate for the fringing pattern affecting the CCD at longer wavelengths. Both night (twilight flat fields) and day time calibration frames (bias,

dome flat fields) were acquired. Unfortunately, due to the presence of clouds both at the beginning and at the end of the night no standard star observations were acquired. As a reference for the photometric calibration we then used the closest in time zero points regularly measured using Landolt stars (Landolt 1983) as part of the instrument calibration plan and available in the photometry calibration database maintained by the *NTT/SUSI2* team. According to the zero point trending plots [1], we estimate a conservative uncertainty of $\sim 0.1$ magnitudes on the values extrapolated to the night of our observations.

### 2.2. Infrared observations

1WGA J1713.4−3949 was observed on May 23rd and 24th 2006 at the ESO Paranal Observatory with *NAos COnica* (*NACO*), the adaptive optics (AO) imager and spectrometer mounted at the *VLT* Yepun telescope. In order to provide the best combination between angular resolution and sensitivity, we used the S27 camera with a pixel scale of 0.″027 (28″ × 28″ field of view). As a reference for the AO correction we used the *GSC-2* star S230012111058 ($V = 14.3$), positioned 11.″5 away from our target, with the *VIS* (4500−10000 Å) dichroic element and wavefront sensor.

Observations were performed in the H and K$_s$ bands. To allow for subtraction of the variable IR sky background, each integration was split in sequences of short randomly dithered exposures with Detector Integration Times (DIT) of 24 s and 5 exposures (NDIT) along each node of the dithering pattern. The *NACO* observations log is summarised in the second half of Table 1. For all observations, the seeing conditions were on average below $\sim 0.″8$. Unfortunately, since the target was always observed at the end of the night, the airmass was always above 1.4. Sky conditions were photometric in both nights. On the first night, the second and third K$_s$-band exposure sequence were aborted because the very high airmass prevented Because of their worse image quality and their much lower signal–to–noise, these data are not considered in the following analysis. The K$_s$-band exposure sequence obtained on the second night was interrupted despite of the very good seeing because of the incoming twilight. Thanks to the combination of good seeing and low airmass, the H-band exposure is the one with the best image quality. Night (twilight flat fields) and day time calibration frames (darks, lamp flat fields) were taken daily as part of the *NACO* calibration plan. Standard stars from the Persson et al. (1998) fields were observed in both nights for photometric calibration.

---

[1] http://www.ls.eso.org/lasilla/sciops/ntt/susi/docs/susiCounts.html

**Table 1.** Log of the *NTT*/*SUSI2* (first half) and *VLT*/*NACO* (second half) observations of the 1WGA J1713.4−3949 field. Columns report the observing epoch, the filter, the total integration time, and the average seeing and airmass.

| yyyy-mm-dd | Filter | T (s) | Seeing (") | Airmass |
|------------|--------|-------|------------|---------|
| 2004-06-13 | B  | 3200 | 1.14 | 1.07 |
| 2004-06-13 | V  | 6400 | 1.12 | 1.03 |
| 2004-06-13 | I  | 3150 | 1.0  | 1.16 |
| 2006-05-24 | Ks | 1800 | 0.66 | 1.45 |
| 2006-05-24 | Ks | 360  | 0.95 | 1.70 |
| 2006-05-24 | Ks | 600  | 0.78 | 1.81 |
| 2006-05-25 | H  | 2400 | 0.62 | 1.42 |
| 2006-05-25 | Ks | 1200 | 0.40 | 1.74 |

## 2.3. Data reduction

The *NTT*/*SUSI2* data were reduced using standard routine available in the `MIDAS` data reduction package[2]. After the basic reduction steps (hot pixels masking, removal of bad CCD column, bias subtraction, flat field correction), single science frames were combined to filter cosmic ray hits and to remove the fringing patterns in the I-band. The astrometry was computed using the coordinates and positions of 61 stars selected from the *2MASS* catalogue (Skrutskie et al. 2006). For a better comparison with the *VLT*/*NACO* IR images, the I-band image was taken as a reference. The pixel coordinates of the *2MASS* stars (all non saturated and evenly distributed in the field) were measured by fitting their intensity profiles with a Gaussian function using the `GAIA` (`Graphical Astronomy and Image Analysis`) tool[3]. The fit to celestial coordinates was computed using the `Starlink` package `ASTROM`[4]. The rms of the astrometric fit residuals was ≈ 0.″09 per coordinate. After accounting for the 0.″2 **conservative** astrometric accuracy of *2MASS* (Skrutskie et al. 2006), the overall uncertainty to be attached to our astrometry is finally 0.″24.

The *VLT* data were processed through the ESO *NACO* data reduction pipeline[5]. For each band, science frames were reduced with the produced master dark and flat field frames and combined to correct for the exposure dithering and to produce cosmic-ray free and sky-subtracted images. The photometric calibration was applied using the zero point provided by the *NACO* pipeline, computed through fixed aperture photometry. The astrometric calibration was performed using the same procedure described above. However, since only five *2MASS* stars are identified in the narrow *NACO* S27 camera field of view, we computed the astrometric solution using as a reference a set of 23 secondary stars found in common with the *SUSI2* I-band image, calibrated using *2MASS*. The rms of the astrometric fit residuals was then ≈ 0.″06 per coordinate. By adding in quadrature the rms of the astrometric fit residuals of the *SUSI2* I-band image and the average astrometric accuracy of *2MASS* we thus end up with an overall accuracy of 0.″25 on the *NACO* image astrometry.

## 3. Data analysis and results

### 3.1. Astrometry

We derived the coordinates of 1WGA J1713.4−3949 through the analysis of unpublished *Chandra* observations. The field of 1WGA J1713.4-3949 was observed on April 19th 2005 with the *ACIS/I* instrument for 9.7 ks. Calibrated (level 2) data were retrieved from the *Chandra* X-ray Center Archive and were analysed using the `Chandra Interactive Analysis of Observations` software (`CIAO v3.3`). In order to compute the target position, we performed a source detection in the 0.5-10 keV energy range using the `wavdetect` task. The source coordinates turned out to be $\alpha(J2000) = 17^h13^m28.32^s$, $\delta(J2000) = -39°49'53''.34$, with a nominal uncertainty of $\sim 0.''8$ (99% confidence level)[6]. The identification of a field X-ray source with the bright star HD 322941 at a position consistent with the one listed in the Tycho Reference Catalog (Høg et al. 2000) confirmed the accuracy of the nominal *Chandra* astrometric solution. Unfortunately, since no other field X-ray source could be unambiguously identified with catalogued objects, it was not possible to perform any boresight correction to the *Chandra* data in order to improve the nominal astrometric accuracy.

The computed 1WGA J1713.4−3949 position is shown in Fig. 1, overplotted on the *NTT*/*SUSI2* I-band and on the *VLT*/*NACO* H-band images. In the former (Fig.1-left) a faint and patchy object is clearly detected northeast of the *Chandra* error circle (I= 23.5 ± 0.3) and a fainter one (I= 24.3 ± 0.4) is possibly detected south of it. However, in both cases their patchy structure makes it difficult to determine whether their are single, or blended with unresolved field objects. No other object is detected within or close to the *Chandra* error circle down to B∼26, V∼26.2 and I∼24.7 (3σ). However, due to the better seeing conditions (see Table 1) and to the sharper angular resolution, five objects are clearly detected in the *VLT*/*NACO* image (Fig. 1-right). Of these, object 413 falls within the *Chandra* error circle. A sixth fainter object (479) is possibly detected, albeit at very low significance. They are all point-like and compatible with the on-axis *NACO* PSF. Objects 401 and 403 are identified with the two faint objects detected in the *NTT*/*SUSI2* I-band image northeast and southeast of the *Chandra* error circle, respectively. The former might be actually a blend of objects 401 and 400, whose angular separation (≈ 0.″6) is smaller than the PSF of the *NTT*/*SUSI2* image. We thus take the measured

[2] http://www.eso.org/sci/data-processing/software/esomidas/

[3] star-www.dur.ac.uk/ pdraper/gaia/gaia.html

[4] http://star-www.rl.ac.uk/Software/software.htm

[5] www.eso.org/observing/dfo/quality/NACO/pipeline
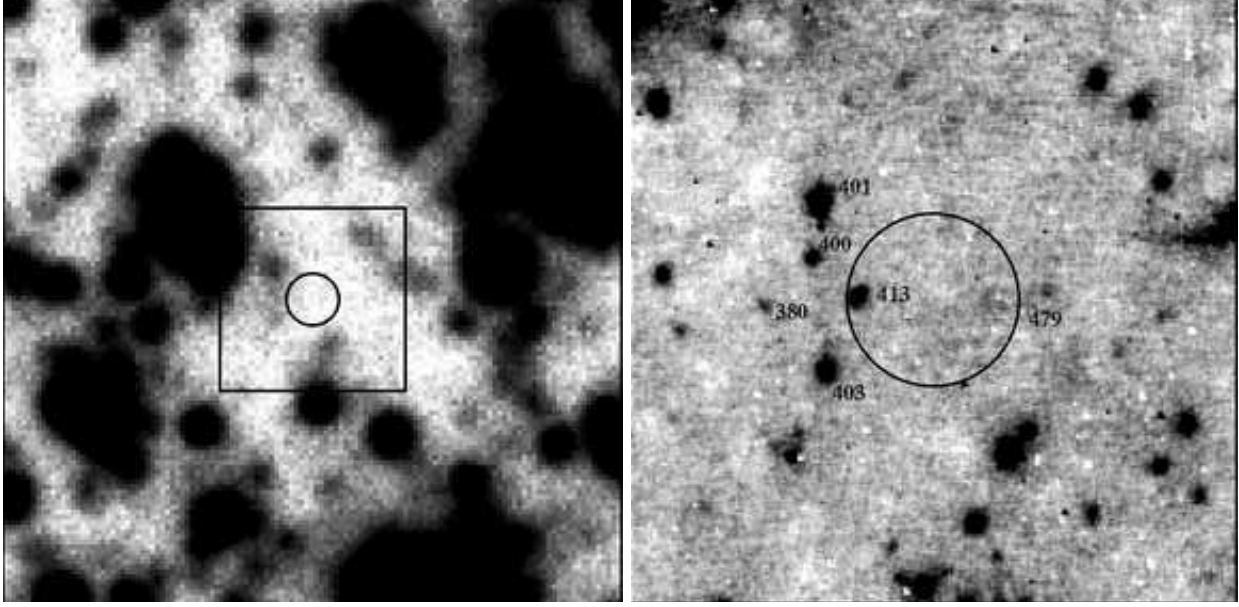
[6] http://cxc.harvard.edu/cal/ASPECT/celmon/

**Fig. 1.** (left) $20'' \times 20''$ *NTT/SUSI2* I-band of the 1WGA J1713.4−3949 field. (right) $6'' \times 6''$ *VLT/NACO* H-band image of the same field. The area corresponds to the square overplotted on the left hand side image. The circle marks the *Chandra* position of the X-ray source, where the radius $(0''.85)$ accounts both for the intrinsic absolute accuracy of the *Chandra* coordinates (99% confidence level) and for the uncertainties of our astrometric calibration (see Sect. 2.3). Possible counterparts are labelled on the right hand side image, with object 479 detected only at $< 5\sigma$.

**Table 2.** *VLT/NACO* H and $K_s$-band photometry and colour of the candidate counterparts of 1WGA J1713.4−3949.

| ID | H | $K_s$ | $H-K_s$ |
|-----|------------------|------------------|------------------|
| 380 | $19.75 \pm 0.14$ | $19.32 \pm 0.11$ | $0.43 \pm 0.18$ |
| 400 | $18.98 \pm 0.13$ | $18.49 \pm 0.09$ | $0.49 \pm 0.16$ |
| 401 | $17.82 \pm 0.13$ | $17.32 \pm 0.08$ | $0.50 \pm 0.15$ |
| 403 | $18.47 \pm 0.13$ | $17.87 \pm 0.08$ | $0.60 \pm 0.15$ |
| 413 | $18.63 \pm 0.13$ | $18.31 \pm 0.09$ | $0.33 \pm 0.16$ |
| 479 | $20.34 \pm 0.15$ | $19.61 \pm 0.12$ | $0.73 \pm 0.20$ |

magnitude (I= $23.5 \pm 0.3$) of object 401 with caution. All the objects detected in the *NACO* H-band image are also detected in the longest 1200 and 1800 s $K_s$-band ones (see Table 1).No other object is detected close to the *Chandra* error circle down to H∼21.3 and $K_s$ ∼20.5 $(3\sigma)$.

### 3.2. Photometry

We computed objects magnitudes in the *NACO* images through PSF photometry using the suite of tools `Daophot`(Stetson 1992) and applying the same procedures described in Zaggia et al. (1997) and applied in Mignani et al. (2007a) and De Luca et al. (2008). Since the *NACO* PSF is largely oversampled, we re-sampled the images with a $3 \times 3$ pixels window using the `swarp` program[7] to increase the signal–to–noise ratio. As a reference for

our photometry we used the co-added and re-sampled H-band image to create a master list of objects, which we registered on the $K_s$-band one and used as a mask for the object detection. For each image, the model PSF was calculated by fitting the profile of a number of bright but non-saturated reference stars in the field and used to measure the objects fluxes at the reference positions. Our photometry was calibrated using the zero points provided by the *NACO* pipeline after applying the aperture correction, with an attached errors of ∼ 0.13 and ∼ 0.08 magnitudes in H and $K_s$, respectively. Single band catalogues were then matched and used as a reference for our colour analysis. The IR magnitudes of our candidates are listed in Tab. 2. We used the $K_s$-band photometry performed on the two consecutive nights to search for variability on time scales of hours. However, none of our candidates shows flux variations larger than 0.1 magnitudes, which is consistent with our photometric errors. Fig. 2 shows the H,H-$K_s$ colour magnitude diagram (CMD) for our candidates as well as for all objects detected in the field. None of the candidates is characterised by peculiar colours with respect to the main sequence of the field stellar population, which suggest that they are main-sequence stars.

### 4. Discussion

To determine whether one of the detected objects is the IR counterpart to 1WGA J1713.4−3949, we investigated how their observed properties fit with different scenarios.

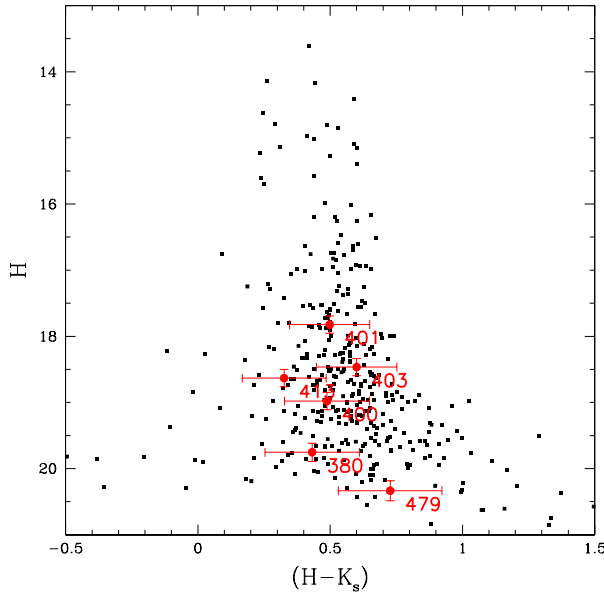---

[7] http://terapix.iap.fr/

**Fig. 2.** H,H-K$_s$ CMD of all stars detected in the *VLT/NACO* field. All candidates identified in Fig. 1 are marked in red and labelled accordingly. No interstellar extinction correction has been applied.

### 4.1. A binary system

If our candidates are stars, we considered the possibility that one of them is the companion of the 1WGA J1713.4−3949 neutron star. Their observed colours are quite red (0.4< H-K$_s$ <0.7), which suggests that they might be intrinsically red late-type stars. To be compatible with the observed range of H-K$_s$ (Ducati et al. 2001), e.g. an M-type main sequence star should be reddened by an amount of interstellar extinction corresponding to an $N_H \sim 10^{22}$ cm$^{-2}$ (Predhel & Schmitt 1995). This value is compatible with the largest values obtained from the spectral fits to 1WGA J1713.4−3949 (Lazendic et al. 2003; Cassam-Chenaï et al. 2004). For the originally proposed 1WGA J1713.4−3949 distance of 6 kpc (Slane et al. 1999) an M-type star with such an high extinction should be at least ∼0.7 magnitudes fainter than our faintest candidate (object 479). An early to mid M-type star would be compatible with the revised distance of $1.3 \pm 0.4$ kpc (Cassam-Chenaï et al. 2004) but it would be detected in our *NTT/SUSI2* image at I∼ 20.2 − 21.7. Thus, we conclude that if our candidates are stars none of them can be associated with 1WGA J1713.4−3949. Our optical/IR magnitude upper limits only allow an undetected companion of spectral type later than M.

### 4.2. An isolated neutron star

If 1WGA J1713.4−3949 is indeed an INS, we can then speculate if one of our candidates is the neutron star itself. Due to the paucity of the neutron stars observed in the IR (e.g. Mignani et al. 2007b) and to the lack of well-defined spectral templates, it is very difficult to estimate

their expected IR brightness. This is even more difficult for the CCO neutron stars, none of which has been unambiguosuly identified so far (e.g. De Luca 2008). In the best characterised case of rotation-powered neutron stars one can deduce that the magnetospheric IR and X-ray luminosities correlate (Mignani et al. 2007b; Possenti et al. 2002). By assuming, e.g. a blackbody plus power law X-ray spectrum for 1WGA J1713.4−3949 (Lazendic et al. 2003; Cassam-Chenaï et al. 2004) we then scaled the magnetospheric IR-to-X-ray luminosity ratio of the Vela pulsar, taken as a reference because of its comparable age ($\sim 10$ kyears). After accounting for the corresponding interstellar extinction we thus estimated K$_s \sim 19.7$ for 1WGA J1713.4−3949, i.e. similar to the magnitude of object 479 (K$_s \sim 19.6$). Since also the magnetospheric optical and X-ray luminosities correlate (e.g., Zharikov et al. 2004), we similarly estimated B≈ 28.3 for 1WGA J1713.4−3949 which, however, is below our *NTT/SUSI2* upper limit (B≥26). Thus, a neutron star identification can not be firmly excluded.

### 4.3. A fossil disk

As discussed in Sect.1, some CCO models invoke low-magnetised INSs surrounded by fallback disks. So, the last possibility is that we detected the IR emission from such a disk. We note that the IR-to-X-ray flux ratio for 1WGA J1713.4−3949 would be $\approx 10^{-3} - 10^{-2}$, i.e. much larger than that estimated for the anomalous X-ray pulsar 4U 0142+61 (Wang et al. 2006), the only INS with evidence of a fallback disk. However, we can not a priori rule out the fallback disk scenario. We computed the putative disk emission using the model of Perna et al. (2000), which accounts for both for the contribution of viscous dissipation as well as that due to reprocessing of the neutron star X-ray luminosity. As a reference, we assumed the X-ray luminosity derived for the updated distance of $1.3 \pm 0.4$ kpc (Cassam-Chenaï et al. 2004). For a nominal disk inclination angle of 60° with respect to the line of sight, the unknown model parameters are the disk inner and outer radii ($R_{in}$,$R_{out}$), and accretion rate ($\dot{M}$). We thus iteratively fitted our data for different sets of the model parameters. For the dimmest candidate we found that the IR fluxes would be consistent with a spectrum of a disk ($R_{in} = 0.28 R_{\odot}$, $R_{out} = 1.4 R_{\odot}$) whose emission is dominated by the reprocessed neutron star X-ray luminosity (Fig. 3), similarly to the case of 4U 0142+61. However, such a disk should be detected in the I band, with a flux $\sim 1.5$ magnitude above our measured upper limit, as shown in Fig. 3. The overprediction of the optical flux is even more dramatic for a disk that fits the brighter counterparts. We thus conclude that, if the neutron stra has a disk, it was not detected by our observations.

## 5. Conclusions

We performed deep optical and IR observations of the CCO 1WGA J1713.4−3949 in the G347.3-0.5 SNR, the
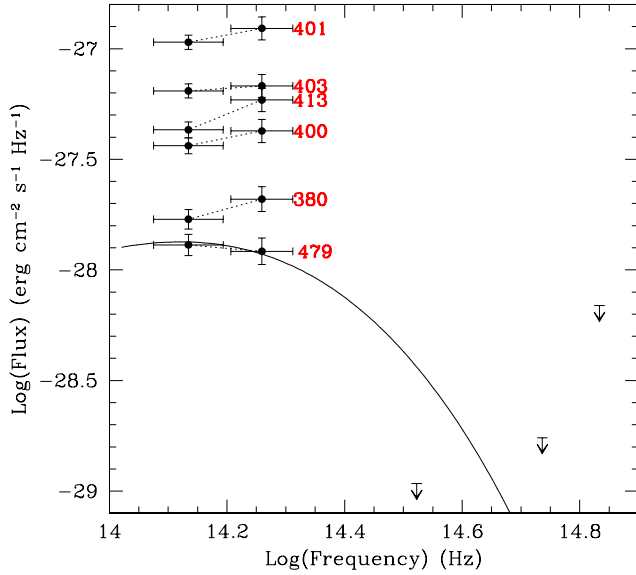
**Fig. 3.** Dereddened IR spectra of the 1WGA J1713.4−3949 candidate counterparts. Dotted lines are drawn for guidance. The BVI bands upper limits are indicated. The solid line is the best fitting disk spectrum ($R_{in} = 0.28R_\odot$, $R_{out} = 1.4R_\odot$) for object 479.

first ever performed for this source, with the *NTT* and the *VLT*. We detected a few objects close to the derived *Chandra* X-ray error circle. However, if they are stars the association with the CCO would not be compatible with its current values of distance and hydrogen column density. Similarly to the cases of the CCOs in PKS 1209−51, Puppis A (Wang et al. 2007), Cas A (Fesen et al. 2006) and RCW 103 (De Luca et al. 2008), our results argue against the presence of a companion star, unless it is later than M-type, and favour the INS scenario. The identification of the faintest candidate with the neutron star itself can not be firmly excluded, while the identification with a fallback disk is ruled out by its non-detection in the I band. Thus, we conclude that the 1WGA J1713.4−3949 counterpart is still unidentified. Deeper optical/IR observations are needed to pinpoint new candidates. Although the source is apparently steady in X-rays, flux variations as observed in the RCW 103 CCO (Gotthelf et al. 1999) can not be a priory excluded. A prompt IR follow-up would then increase the chances to identify the 1WGA J1713.4−3949 counterpart.

## References

Cassam-Chenaï, G., Decourchelle, A., Ballet, J., Sauvageot, J.-L., Dubner,G., et al., 2004, A&A, 427, 199

De Luca, A., Caraveo, P. A., Mereghetti, S., Tiengo, A., Bignami, G. F., 2006, Science, 313, 814

De Luca, A., Mignani, R.P., Zaggia, S., Beccari, G., Mereghetti, S., et al., 2008, ApJ, in press, [arXiv:0803.2885]

De Luca, A., 2008, in Proc. of 40 Years of Pulsars: Millisecond Pulsars, Magnetars and More, AIP, 938, 311

Ducati, J.R., Bevilacqua, C.M., Rembold, S.B., Ribeiro, D., 2001, ApJ, 558, 309

Fesen, R. A., Pavlov, G. G., Sanwal, D. 2006, ApJ, 636, 848

Gotthelf, E. V., Petre, R., Vasisht, G., 1999, ApJ, 514, L107

Gotthelf, E. V., Halpern, J.P., 2007, ApJ, 664, L35

Halpen, J.P., Gotthelf, E. V., Camilo, F., Seward, F.D., 2007, ApJ, 665, 1304

Høg E., Fabricius C., Makarov V.V., et al., 2000, A&A, 355, L27

Krause, O, Rieke, G.H., Birkmann, S.M., Le Floc'h, E., Gordon, K. D., et al., 2005, Science, 308, 1064

Landolt, A.U., 1983, AJ, 88, 439

Lazendic, J.S., Slane,P.O., Gaensler, B.M., Plucinsky, P.P., Hughes, J.P., 2003, ApJ, 593, L27

Lazendic, J.S., Slane,P.O., Gaensler, B.M., Reynolds, S.P., Plucinsky, P.P., et al., 2004, ApJ, 602, 271

Mignani, R.P., De Luca, A., Zaggia, S., Sester,D., Pellizzoni, A., et al., 2007a, A&A, 473, 833

Mignani, R.P., Perna, R., Rea, N., Israel, G.L., Mereghetti, S., et al. 2007b, A&A, 471, 265

Pavlov, G. G., Zavlin, V.E., Aschenbach. B., Trümper,J., Sanwal, D., 2000, ApJ, 531, L35

Pavlov, G.G., Sanwal, D., Garmire, G.P., Zavlin, V.E., 2002 in Proc. of Neutron Stars in Supernova Remnants, ASP Conference Series, Vol. 271, p.247

Pavlov, G. G., Sanwal, D., Teter, M. 2004, IAU Symp. Vol 218, 239

Perna, R., Hernquist, L., & Narayan, R. 2000, ApJ, 541, 344

Pfeffermann, E., Aschenbach, B., 1996, Mpe Report, 263,267

Pizzolato, F., Colpi, M., De Luca, A., Mereghetti, S., Tiengo, A., 2008, ApJ, accepted, [arXiv:0803.1373]

Possenti, A., Cerutti, R., Colpi, M., Mereghetti, S., 2002, A&A, 387, 993

Predehl, P. & Schmitt, J.H.M.M. 1995, A&A 293, 889

Skrutskie, M. F., Cutri, R. M., Stiening, R., Weinberg, M. D., Schneider, S., et al., 2006, AJ, 131, 1163

Slane, P., Gaensler, B. M., Dame, T.M., Hughes, J.P., Plucinsky, P.P., et al., 1999, ApJ, 525, 357

Stetson, P. B. 1992, ASP Conf. Ser. 25: Astronomical Data Analysis Software and Systems I, 25, 297

Wang, Z., Chakrabarty, D., Kaplan, D. L. 2006, Nature, 440, 772

Wang, Z., Kaplan, D., Chakrabarty, D., 2007, ApJ, 655, 261

Zaggia, S. R., Piotto, G., & Capaccioli, M. 1997, A&A, 327, 1004

Zharikov, S. V., Shibanov, Yu. A., Mennickent, R. E., Komarova, V. N., Koptsevich, A. B., et al., 2004, A&A, 417, 1017